Nuclear Engineering and Technology 49 (2017) 1157–1164

Contents lists available at ScienceDirect

Nuclear Engineering and Technology

journal homepage: www.elsevier.com/locate/net

Original Article

Clustering and traveling waves in the Monte Carlo criticality simulation of decoupled and confined media

Eric Dumonteil [a, *], Giovanni Bruna [a], Fausto Malvagi [b], Anthony Onillon [a], Yann Richet [a]

[a] Institut de Radioprotection et de Sûreté Nucléaire, IRSN/PSN-EXP/SNC, 92262, Fontenay-aux-Roses, France
[b] Den-Service D'études des Réacteurs et de Mathématiques Appliquées (SERMA), CEA, Université Paris-Saclay, F-91191, Gif-sur-Yvette, France

ARTICLE INFO

Article history:
Received 3 June 2017
Received in revised form
19 July 2017
Accepted 26 July 2017
Available online 3 August 2017

Keywords:
Monte Carlo
Criticality
Biases
Clustering
Traveling waves

ABSTRACT

The Monte Carlo criticality simulation of decoupled systems, as for instance in large reactor cores, has been a challenging issue for a long time. In particular, due to limited computer time resources, the number of neutrons simulated per generation is still many order of magnitudes below realistic statistics, even during the start-up phases of reactors. This limited number of neutrons triggers a strong clustering effect of the neutron population that affects Monte Carlo tallies. Below a certain threshold, not only is the variance affected but also the estimation of the eigenvectors. In this paper we will build a time-dependent diffusion equation that takes into account both spatial correlations and population control (fixed number of neutrons along generations). We will show that its solution obeys a traveling wave dynamic, and we will discuss the mechanism that explains this biasing of local tallies whenever leakage boundary conditions are applied to the system.

1. Introduction

Monte Carlo neutron transport codes [1,2] are often used as a reference tool by the nuclear industry, as the approximations on which they rely to solve the Boltzmann equation in fissile media (the so-called critical Boltzmann equation [3]) are extremely sparse. Their growing use in the past few decades is strongly correlated to the increase of computer resources and now ranges from nuclear fuel cycle studies to criticality safety assessment and reactor physics simulations. However, in this last application, and especially in the case of large reactor cores or loosely coupled systems [4,5], a strong undersampling effect biases the estimates of the variance of flux-based quantities [6–10]. Worse, in a work inspired by recent developments in population ecology [11–14], Dumonteil, Mazzolo and Zoia have shown that non-Poisson spatial fluctuations were caused by a neutron clustering phenomenon [15–18]: even for intermediate or high numbers of simulated neutrons, those fluctuations can make it hard to estimate flux-based standard deviations. The very first description of this mechanism typical of birth–death processes dates back to the 1980s, when Cox and Griffeath [19] showed that the spatial correlations affecting some branching processes evolving in infinite media in dimension 1 or 2 were diverging in amplitudes, while in dimension 3 those spatial correlations would saturate. Later on, while being translated from the field of probabilities to the fields of population ecology (describing spatial patterns appearing in water column plankton [11] or describing bacterial growth in Petri dishes [13,14]), neutron transport [15,16], and statistical mechanics [17,18], this process was referred to as clustering or Brownian bugs, whether it be for finite or infinite media in any dimension and with different kinds of boundary conditions. In the present paper, we will show that space-dependent biases observed while simulating the neutron transport in decoupled systems find their origin in these spatial correlations, when leakage boundary conditions are employed. Section 2 will discuss the phenomenology of these biases on a commercial reactor benchmark, and on a simplified model grasping its main characteristics [the mass-preserved one-dimensional (1D) binary branching Brownian motion on a segment with Dirichlet boundary conditions]. In Section 3 we will build a functional equation modeling the simplified case, based on a generalized Fisher equation with time-dependent coefficients that accounts for population control and which incorporates spatial correlations. In Section 4 we will rely on an asymptotic analysis to establish a deep connection between traveling waves proper to quadratic terms in the neutronic field equation and clustering. In particular, we will show that the neutron clusters trigger a traveling

* Corresponding author.
E-mail address: eric.dumonteil@irsn.fr (E. Dumonteil).

http://dx.doi.org/10.1016/j.net.2017.07.011

wave dynamic on the flux causing the bias on local tallies. Some numerical solutions of this equation retrieved under simplifying hypotheses will be compared to the numerical findings of the first section. Conclusions will be drawn in the final section.

2. Biases associated to the Monte Carlo simulation of large reactor cores

2.1. Commercial reactor critical benchmark

The Expert Group on Advanced Monte Carlo Techniques belongs to the Working Party on Nuclear Criticality Safety of the OECD Nuclear Energy Agency. Its aim is, amongst others, to guide Monte Carlo criticality practitioners through finding their ways in defining the most appropriate simulation parameters, so as to minimize biases in the Monte Carlo estimate of different local quantities or in the estimate of their variances. This group, as well as recent work, has pointed out strong bias in both the estimate of the flux and its variance, which depends on the spatial position of the tally volume [20,21]. This bias is prone to develop in particular for loosely coupled systems. Thus, a benchmark named R1 is currently under study, which proposes to tally the flux in different radial zones of a critical commercial reactor [22]. This reactor has been simulated with the MORET 5.B.2 Monte Carlo code [23], exploiting a quarter symmetry. Axially averaged fluxes are presented on the left part of Fig. 1 and the associated "apparent" 1-σ error bars are provided by the left plot of Fig. 2 (these error bars are calculated by the Monte Carlo code using the central limit theorem). As expected, the highest uncertainties are located in low flux regions, where neutrons leak out of the core. Surprisingly enough, though, the "true" error bars given by the right plot of Fig. 2 exhibit spatial patterns: these errors seem to be big near the leaking boundaries of the reactor core but are also close to the reflecting boundaries and at the center of the core. Such nontrivial spatial patterns are even more striking on the right plot of Fig. 1, where the undersampling bias is estimated and is shown to be bigger at the center of the core, and close to the leaking boundaries. In particular, the flux is overestimated near the leaking edges and is underestimated at the center. Also, the amplitude of this bias, be it positive or negative, seems to be inversely proportional to the number of neutrons per generation, as revealed by Fig. 3 In the following parts of this paper, we will try to model this very last phenomenon, also reported by many authors and papers.

2.2. Mass preserving branching Brownian motion on a 1D confined medium with Dirichlet boundary conditions

In order to explain these observations, different capabilities of the MORET 5.B.2 Monte Carlo code were successively disabled (simplified geometry, one group cross-sections, etc.) to grasp the phenomenology discussed in the present paper with the simplest model. In this respect it appeared that a mass-preserving binary branching Brownian motion [19,24,25] on a segment (of half length L arbitrarily set to 20) with Dirichlet (leakage) boundary conditions allowed to observe precisely an underestimation of the flux in the central region while reproducing an overestimation of the flux close to the boundaries. It is worth noting that such a modeling is more suited to Monte Carlo dynamic simulations (which make use of an algorithmic loop over time steps instead of a loop over neutron generations): for that reason a methodology to model generation-based simulations directly, instead of time-dependent problems, was proposed in a very recent work [26]. However, for the particular phenomenon described in this paper no significant differences were observed between criticality and dynamic simulations: continuous time processes will be used as a means to draw conclusions that apply to both processes. The mass-preserving mechanism used in the simulations is fully described [27,28,18]. It is based on a combination between splitting and Russian roulette techniques: each time a particle is captured by a physics process, another is picked randomly and split, while each time a fission occurs, a randomly picked particle is Russian rouletted. The diffusion coefficient D was set to 1, while the binary process was such that the capture cross-section γ was equal to the two-daughter particles fission cross-section β, and both were set to 0.1. Typical realizations of such a process are provided in Fig. 4. As expected, the top plot of this figure highlights a strong particle clustering mechanism [16], and reveals that, after a short time, only one cluster remains [17]. Interestingly enough, though, looking at this process on a large time window (bottom plot), a qualitative view of the problem under consideration emerges: when only one cluster of particles strikes one of the boundaries while wandering around, the constraint on the overall mass N of our mass-preserving process refrains the particle cluster from leaking out of the system, the splitting rate increases dramatically until the cluster is "reflected" to the other side of the system. Therefore the Dirichlet boundary conditions cannot be properly taken into account. When the system is not prone to trigger a clustering effect (i.e., for coupled

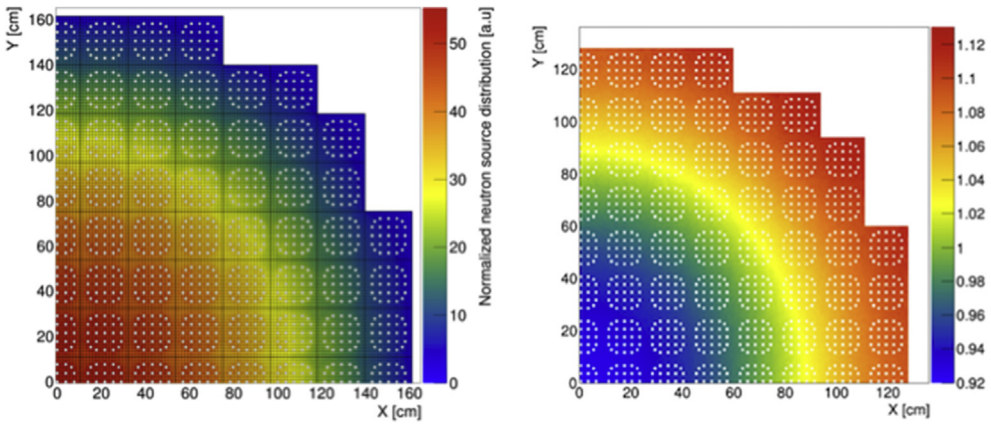

Fig. 1. MORET 5.B.2 simulation of the R1 OECD/NEA benchmark: axially averaged fluxes with 10^4 active cycles of 10^4 neutrons (left plot). Ratio of the axially averaged fluxes between a simulation with 10^6 active cycles of 10^2 neutrons and a simulation with 10^2 active cycles of 10^6 neutrons (right plot).

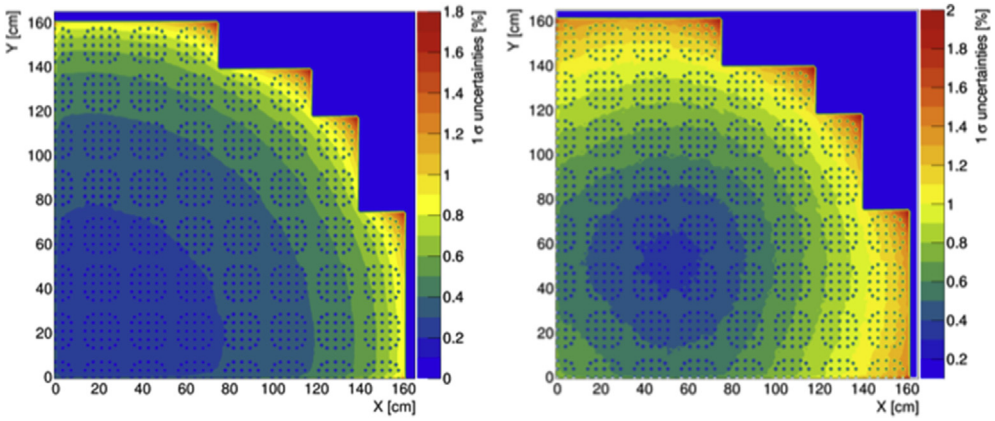

Fig. 2. MORET 5.B.2 simulation of the R1 benchmark with 10^4 active cycles of 10^4 neutrons: 1-σ error bars ("apparent errors") on the axially averaged fluxes (left plot) and 1-σ error bars ("true errors" estimated by independent simulations) on the axially averaged fluxes with 10^4 active cycles of 10^4 neutrons (right plot).

configurations, with dominant ratio sensitively less than 1), the splitting mechanism that compensates leakages picks particles according to a converged eigenvector and the bias disappears. Fig. 5 sums up these discussions: the typical cosine shape of the mean flux solution of the one-group Boltzmann critical equation for a slab geometry is progressively distorted following a flat distribution at the center with a strong decay near the extremities, when the number of simulated particles gets smaller. For a small number of particles ($N = 50$), the cluster density profile has been numerically calculated by averaging $\langle x(t) - \langle x(t)\rangle\rangle_t$ over $\Delta t = 1000$ (a.u.), where $\langle x(t)\rangle$ is the average over all realizations of the process at a given time. The typical resulting profile of the clusters given in Fig. 6 exhibits exponentially decaying tails with a cutoff at ± 40, corresponding to the maximum distance between two particles. This typical profile has a spatial extension proportional to the number of particles: when this extension is smaller than the typical size of the system, the clusters wander around randomly so as to produce the flat structures for the mean flux discussed above.

3. The time-dependent generalized Fisher equation with population control

In this section we will build a stochastic model for our process (mass-preserved binary branching Brownian motion on a segment) and discuss some of its analytical solutions, obtained under simplifying hypotheses, in the case of Dirichlet or Neumann boundary conditions.

3.1. Generalized Fisher equation in the context of population ecology

The key ingredient used as a starting point of our modeling is the Fisher equation [29,30], also known in population biology as the spatial logistic equation, or in theoretical physics as the KPP (Kolmogorov–Petrovskii–Piskunov) equation. To build this equation, one starts with the diffusion equation

$$\partial_t \phi = D\partial_x^2 \phi + (\beta - \gamma)\phi, \tag{1}$$

where ϕ is a density,[1] D is the diffusion coefficient, β is a reproduction rate, and γ is a disappearance rate. The Fisher equation is a diffusion equation with a supplementary quadratic term in the flux. It takes the following form

$$\partial_t \phi = D\partial_x^2 \phi + (\beta - \gamma)\phi + \lambda\phi^2, \tag{2}$$

where the coefficient λ is a saturation rate in front of ϕ^2. Indeed, depending on the sign of λ, this saturation rate can be seen as imposing either a maximal threshold value for the flux (for negative λ) above which negative counter-reaction will take place, or a minimal threshold value for the flux (for positive λ), below which positive counter-reaction will develop. To give a concrete example, in population ecology β and γ can be interpreted, respectively, as the birth and death rates of a given species, whereas λ might be interpreted as a saturation due to the competition for resources between individuals of this species. The squared flux term arises from the fact that local interactions between individuals are combinatorial: the survival of an individual in x depends on the number of individuals in the vicinity of x. Therefore the death probability has to be adjusted by a saturation term proportional to the number of pairs of individuals $\binom{N(x)}{2}$ in $[x, x+dx]$ (where $N(x) = \phi(x)dx$ is the number of individuals in $[x, x+dx]$), hence being quadratic in the ϕ-field.

When the competition term depends on the local density of individuals, the clustering effect described in Section 1 cannot be neglected anymore as it affects the density itself. Therefore the

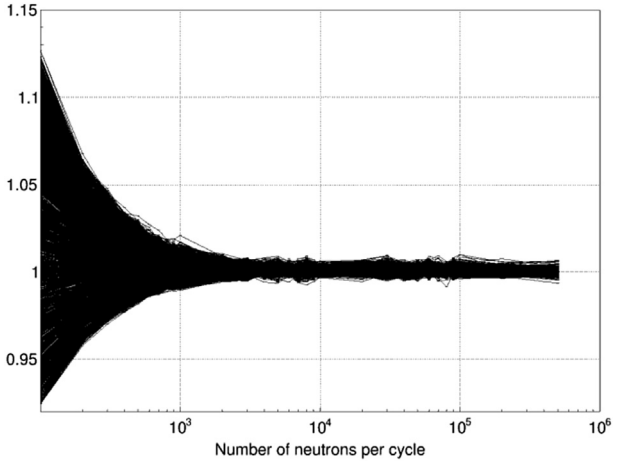

Fig. 3. MORET 5.B.2 simulation of the R1 benchmark with 10^4 active cycles: axially integrated flux in each pin-cell as a function of the number of neutrons per cycle. The fluxes are divided by reference fluxes obtained by simulating 10^6 neutrons per cycle. Fits of flux plots for each pin-cell indicate that the bias is inversely proportional to the number of neutrons per cycle.

[1] In the following we will adopt a convention where the functions variables are implicit in order to lighten the equations. In this case, $\phi = \phi(x, t)$.

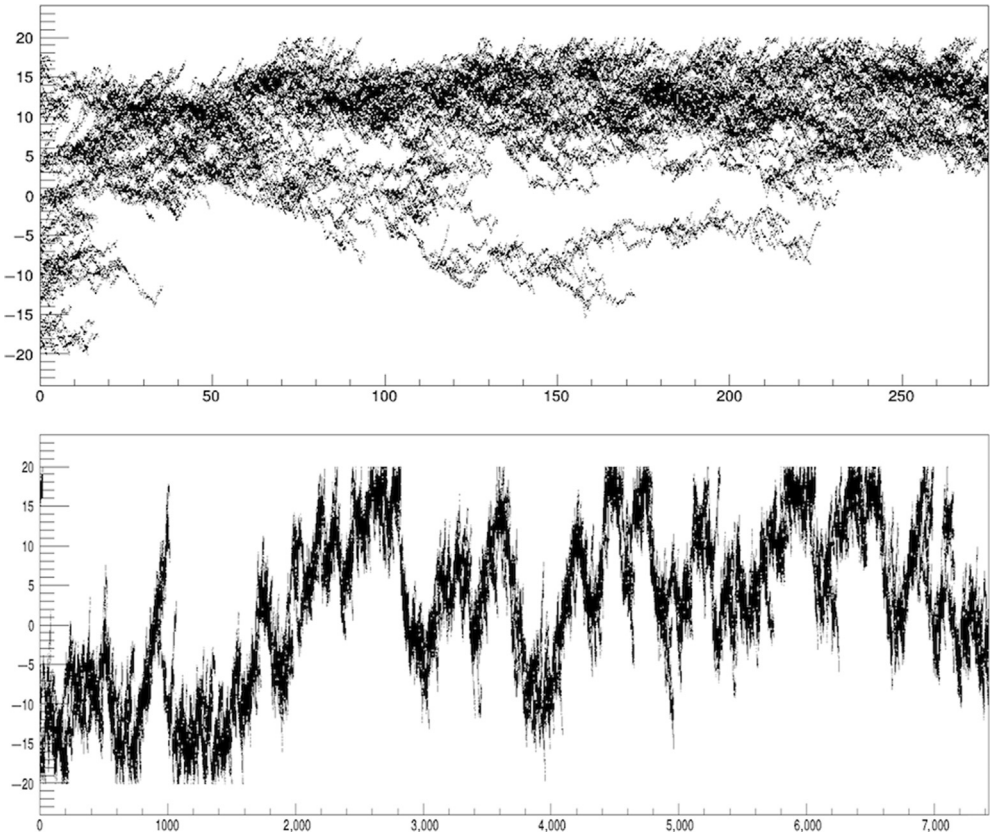

Fig. 4. x positions (x-axis) of the particles versus time t (y-axis) for two realizations of a mass-preserved binary branching Brownian motion on a segment (between −20 and 20) with Dirichlet boundary conditions and with $N = 50$ particles. Top plot: first realization observed between $t = 0$ and $t = 300$, bottom plot: second realization observed between $t = 0$ and $t = 7250$.

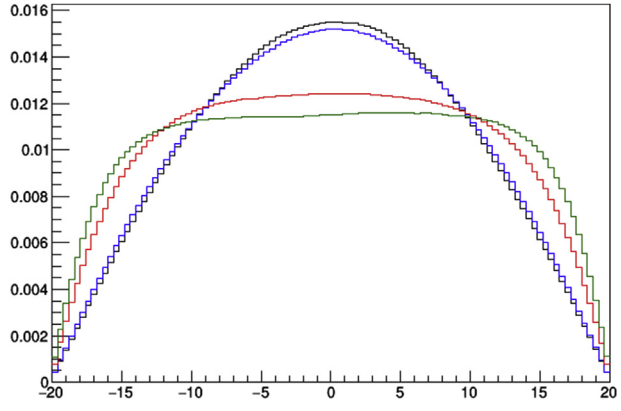

Fig. 5. Normalized particle density—obtained by averaging over $\Delta t = 1000$ (a.u.)—for a mass-preserved binary branching Brownian motion on a segment (between -20 and 20) with Dirichlet boundary conditions and with N particles. Black curve: $N = 1000$, blue curve: $N = 100$, red curve: $N = 10$, green curve: $N = 5$.

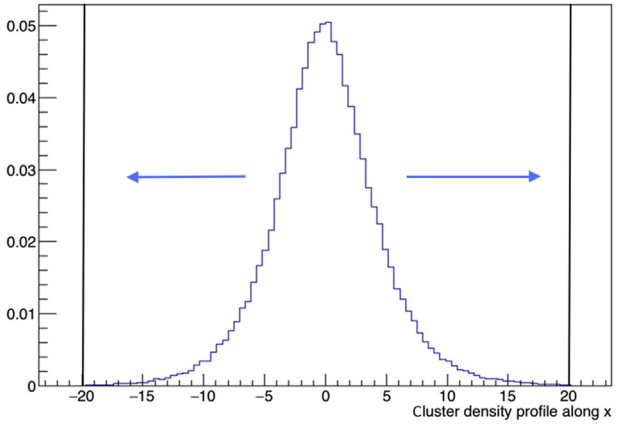

Fig. 6. Normalized cluster density—obtained by averaging over $\Delta t = 1000$ (a.u.)—for a mass-preserved binary branching Brownian motion on a segment (between -20 and 20) with Dirichlet boundary conditions and with $N = 50$ particles.

Poisson spatial distribution of individuals used to build Eq. (2) is no longer true and one has to resort to a generalized Fisher equation (see the pioneer work of Birch and Young [31] for the full development). The generalized Fisher equation

$$\partial_t \phi = D\partial_x^2 \phi + (\beta - \gamma)\phi + \lambda \int dy\, \nu(|x - y|) G(x, y, t), \tag{3}$$

makes use of the pair correlation function G(x,y,t) which is defined such as $G(x, y, t)dxdy$ is the expected number of pair of individuals with one individual in x and the other in y, and of the competition kernel $\nu(r)$ that defines the spatial scale over which the competition occurs.

3.2. Adaptation of the generalized Fisher equation to reactor physics: time-dependent coefficients and population control

The critical Boltzmann equation is commonly used in reactor physics to model the neutron transport in fissile media [3], together with its approximate form, the critical diffusion Eq. (1). In neutron

transport, the $\beta\phi$ and $\gamma\phi$ reaction rates now represent fission and capture events, and are therefore respectively proportional to the fission and capture cross-sections. However, whether it be for reactor physics itself or for the simulation of reactor physics with Monte Carlo neutron transport codes, feedback effects arising from local/global constraints on the neutron population are left aside by the transport/diffusion equation. These feedback effects arise, for example, from:

- spatial and temporal control rod adjustments of the power during the operation of reactor cores. Those adjustments aim for instance at preventing local power excursions.
- the so-called "weight-watching" mechanisms (Russian roulette and splitting) which are used at the end of each cycle (or each time step) of Monte Carlo criticality (or dynamic) simulations to adjust the number of simulated neutrons, so as to prevent any divergence or disappearance of the global population. This mechanism is also referred to as the "renormalization" method in this context.

In both cases—reactor physics or its Monte Carlo simulation—the fundamental ingredient lacking in the transport equation is the introduction of a feedback reaction rate term that.

- depends on the local/global neutron population. This term describes the rate at which local adjustments of the neutron density occur and relates the fission/capture probabilities of a neutron along its path to the local/global neutron densities seen by this neutron. In particular, it shall be sensitive to spatial correlations. The structure of this term is therefore precisely the one discussed in Section 3.1.: $\lambda \int dy\, \nu(|x-y|)G(x,y,t)$; and
- depends on time. As mentioned at the beginning of this section, the local adjustments per unit of time depend on time/generation and the population number is constantly readjusted. In pretty much the same manner as in a work of Newman et al. [32] we can therefore adjust the population by using a time-dependent adjustment coefficient $\lambda(t)$.

In the following, and without loss of generality, we will keep in mind the Monte Carlo criticality simulation of a 1D branching Brownian with $k_{eff}<1$: at each cycle (or similarly for any time), the number of neutrons produced by fission is smaller than the number of neutrons at the beginning of the cycle and the λ coefficient is therefore positive. It represents the splitting mechanism which produces neutrons to compensate for leakages and absorptions. In this case, the competition kernel $\nu(r)$ can be simplified because the spatial range on which the population control is applied does not depend on the distance between neutrons: it is a global constraint on the overall population and will therefore be set to 1 in the following. Also, the population-control criteria can be made explicit by integrating Eq. (3) over the positions between $-L$ and L which gives

$$\lambda(t)=\frac{-\beta+\gamma-D\int_{-L}^{L}dx\,\partial_x^2\phi(x,t)}{\int_{-L}^{L}dx\int_{-L}^{L}dy\,G(x,y,t)}, \tag{4}$$

where we have used the following normalization relation

$$\int_{-L}^{L}dx\,\phi(x,t)=1. \tag{5}$$

In our example with $k_{eff}<1$, this positive coefficient is interpreted as the splitting rate that compensates the neutron loss at each generation. It is consequently proportional to the number of captures (γ) and to the number of leakages $\left(-D\int_{-L}^{L}dx\,\partial_x^2\phi(x,t)\right)$ and is smaller when productions by fission (β) are important. Finally, it is more convenient to use the normalized and centered pair correlation function $g(x,y,t)$ defined as

$$g(x,y,t)=\frac{G(x,y,t)-\phi(x,t)\phi(y,t)}{\phi(x,t)\phi(y,t)}. \tag{6}$$

Upon injection in Eq. (3) we get our equation for the dynamic of a branching Brownian motion in a confined medium with population control

$$\begin{aligned}\partial_t\phi(x,t)&=D\partial_x^2\phi(x,t)+(\beta-\gamma)\phi(x,t)\\&\quad+\lambda(t)\left(1+\int_{-L}^{L}dy\,g(x,y,t)\phi(y,t)\right)\phi(x,t),\end{aligned} \tag{7}$$

together with its limit condition $\phi(\pm L,t)=0$ and with $\lambda(t)$ given by Eq. (4). We also recall here that $g(x,y,t)$ is the normalized and centered pair correlation function of our system.

4. Clustering and traveling waves in bounded domains

The rather intricate form of this generalized Fisher equation with population control does not allow for direct solving as the pair correlation function has not been made explicit. However, surprisingly enough, it is provided in a recent work of De Mulatier et al. [18], where the authors were able to provide an amenable form of the correlation function for branching Brownian motion with population control on bounded domains. In this section we will therefore use an asymptotic analysis of Eq. (7), and we will show that its solution, in the case where the neutron population is small and whenever leakage boundary conditions are used, differs from the "deterministic" one, allowing to understand the cause and the structure of the bias observed in Section 2.

4.1. Large population size

Whenever the neutron population N is very large, we have $g(x,y,t)\to 0$ as the spatial correlations arising from the branching process vanish (see for instance [18,31]. Hence, the pair correlation function G becomes separable in x and y and we have $G(x,y,t)\to\phi(x,t)\phi(y,t)$ so that $\int dy\,G(x,y,t)\to\phi(x,t)$ and $\int dx\int dy\,G(x,y,t)\to 1$. The stationary limit of Eq. (7) takes in this case the very simple form

$$\partial_x^2\phi-\left(\int_{-L}^{L}dx\,\partial_x^2\phi(x)\right)\phi=0. \tag{8}$$

Noticing that $\int_{-L}^{L}dx\,\partial_x^2\phi(x)=\partial_x\phi(x)|_{x=\pm L}$, this equation simplifies to

$$\partial_x^2\phi-\partial_x\phi(x)|_{x=\pm L}\phi=0. \tag{9}$$

In the case of reflecting boundary conditions at each side of the domain, we have to use the Neumann boundary conditions $\partial_x\phi|_{x=\pm L}=0$. Eq. (9) is therefore trivially verified, ensuring that the Monte Carlo criticality renormalization in this case is unbiased.

In the case of absorbing boundary conditions at each side of the domain, we have to use the Dirichlet boundary conditions given by $\phi(x,t)|_{x=\pm L}=0$. Surprisingly enough, this boundary condition applied on a positive and symmetric function ensures that the

coefficient in front of the term linear in ϕ is strictly positive. To go further, as a guess function it is possible to test the cosine solution of the diffusion approximation of the stationary Boltzmann critical equation with leakages. This test function can be written as $\phi(x) = A\,cos\left(\frac{\pi}{2}\frac{x}{L}\right)$, where $A = \frac{\pi}{4L}$ is defined upon normalization of the density function $\phi(x)$. This implies that $\partial_x\phi(x)|_{x=\pm L} = -\frac{\pi^2}{4L^2}$. As a consequence, we have

$$\partial_x^2\phi + \frac{\pi^2}{4L^2}\phi = 0, \tag{10}$$

ensuring that Eq. (9) is verified. The solution of this equation is indeed a cosine, ensuring also that the Monte Carlo criticality renormalization in this case is unbiased. It is noticeable that none of the coefficients of this equation depend on the values of β, γ, or D, and that there is always a solution to this problem, unlike for the critical diffusion equation where a criticality condition linking the geometry and the compositions has to be met. However, this can be understood if we keep in mind that this is precisely the purpose of the renormalization: whatever the parameters characterizing the system, the simulation converges to an unbiased estimate of $\phi(x)$.

4.2. Small population size

If the neutron population N is too small, clusters of neutrons appear (see [16–18] for a precise criterion on N values that trigger the clustering phenomenon). For a long time $t \to \infty$, only one cluster is still alive, with a constant number of neutrons N. This cluster wanders around randomly, with a spatial extension determined by a normalized and centered correlation function that we call $g^\infty(x,y)$. The analytical form of $g^\infty(x,y)$ is given in De Mulatier et al. [18] and its amplitude can be shown to be bounded above by

$$g^\infty(x,y) \leq \frac{2}{3}\frac{\beta}{\gamma}\frac{\nu_2}{N}\frac{L^2}{D}, \tag{11}$$

where ν_2 stands for the mean number of pairs created at each collision. Since we are interested in configurations triggering a strong clustering (i.e., $g^\infty(x,y) \gg 1$), Eq. (11) implies that the renewal time, proportional to N, has to be far smaller than the mixing time proportional to L^2/D. We can therefore conclude that the system size $2L$ has to be big, which also implies that the dynamic of clusters far from the boundaries is the same whether we use Dirichlet or Neumann boundary conditions (leakages or reflections). We will therefore use the same correlation function for both conditions. Finally, for a long time (one cluster) and systems having an important spatial extension, we can also assume that the correlation function only depends on $|x-y|$ so that $g^\infty(x,y) = g^\infty(|x-y|)$. Having all these assumptions in mind, the pair correlation function can be written

$$G(x,y,t) = g^\infty(|x-y|)\phi(x,t)\phi(y,t), \tag{12}$$

and its y-integral over the positions reads

$$\int_{-L}^{+L} dy\, G(x,y,t) = \phi(x,t)\int_{-L}^{+L} dy\, g^\infty(|x-y|)\phi(y,t). \tag{13}$$

Birch and Young [31] show that whenever the spatial correlation function can be approximated by a delta function, this last expression takes the form

$$\int_{-L}^{+L} dy\, G(x,y,t) = \phi(x,t)\int_{-L}^{+L} g^\infty(|r|)dr\phi(x,t). \tag{14}$$

This hypothesis on the structure of the spatial correlation function is relevant for strongly decoupled systems which typical dimensions are order of magnitudes bigger than the typical spatial correlation length. The last expression can then be transformed into

$$\int_{-L}^{+L} dy\, G(x,y,t) = g^\infty\phi(x,t)^2, \tag{15}$$

where we have defined $g^\infty = \int_{-L}^{+L} g^\infty(|r|)dr$. This allows us to rewrite

$$\int_{-L}^{+L} dx \int_{-L}^{+L} dy\, G(x,y,t) = g^\infty \int_{-L}^{+L} dx\, \phi(x,t)^2, \tag{16}$$

so that Eq. (7) becomes

$$\partial_t\phi(x,t) = D\partial_x^2\phi(x,t) + (\beta-\gamma)\phi(x,t) + \left(\frac{-\beta+\gamma-D\partial_x\phi(x,t)|_{x=\pm L}}{\int_{-L}^{+L} dx\, \phi(x,t)^2}\right)\phi(x,t)^2. \tag{17}$$

If we are interested in the dynamic behavior of our system before the cluster reaches the boundaries, the term that accounts for leakages ($D\,\partial_x\phi(x,t)|_{x=\pm L}$) can be neglected compared to $|\beta-\gamma|$ (we suppose that both reaction rates do not have exactly the same value). We can therefore conclude that $\lambda(t) = \lambda = -(\beta-\gamma)/\left(\int_{-L}^{+L} dx\, \phi(x,t)^2\right)$ so that our final equation is given by

$$\partial_t\phi = D\partial_x^2\phi + (\beta-\gamma)\phi - (\beta-\gamma)\frac{\phi^2}{\int dx\, \phi(x,t)^2}, \tag{18}$$

which can be rewritten, after factorization of the linear and quadratic terms in ϕ

$$\partial_t\phi = D\partial_x^2\phi + (\beta-\gamma)\phi\left(1 - \frac{\phi}{\int dx\, \phi(x,t)^2}\right). \tag{19}$$

This equation has a form close to the Fisher equation discussed Section 3, apart from its time-dependent coefficient that ensures the flux normalization. It is called the conserved Fisher equation and provides the full traveling wave dynamic of the neutron flux field, at least before the wave hits the boundaries. Written this way, its meaning is straightforward: as soon as the flux exceeds the time-dependent threshold $\left(\phi > \int dx\, \phi(x,t)^2\right)$, the population control counteracts by Russian roulette to maintain the fixed size of the population. When the flux gets too small (for instance when a cluster reaches the leaking boundary), the splitting of neutrons induces an artificial fission process in the same aim.

The solutions of such an equation are discussed at length [32]. This reference demonstrates in particular that the solutions of the conserved Fisher equations are pseudo-traveling waves. For the

specific case of $D = 0$ (asymptotic limit of small spatial coupling) and for an initial condition being

$$\phi(x,0) = A\exp\Big(-\left|x/\xi_0\right|^{\beta}\Big), \tag{20}$$

with ξ_0 and β being arbitrary parameters, this conserved Fisher equation is analytically amenable and its solution for large t (but before reaching the boundaries) are shown to be

$$\phi(x,t) = \frac{1}{\xi(t)}\left\{\exp\left(\left|\frac{x}{\xi_0}\right|^{\beta} - \left|\frac{\xi(t)}{\xi_0}\right|^{\beta}\right) + 1\right\}^{-1}, \tag{21}$$

with $\xi(t) \sim t^{1/(1+\beta)}$. For $\beta = 1$ the flux provided in Eq. (21) is given in Fig. 7 for different times. Once the pseudo traveling wave has explored the available space, it reaches the boundaries of the domain and stabilizes to an asymptotic shape probably close to Eq. (21). This figure also indicates that the shape of the flux is very similar to the one obtained by the Monte Carlo simulation of a small population of neutrons (see Fig. 5): the density profile of the flux presents a flat structure with fast decaying tails ensuring the Dirichlet boundary condition at the spatial boundaries.

It is interesting to notice that this traveling wave behavior of the flux seems to be triggered by a soliton wave dynamic of the spatial correlation function. Indeed the spatial correlation function describing the cluster has a stationary shape in the long time regime as predicted by [18] and as confirmed by the numerical simulation in Fig. 6. Said in other terms, the neutron cluster behaves itself like a soliton wave: when integrated through configurations it gives rise to the symmetric traveling wave describing the neutron field. This kind of behavior is called the hierarchy horror: the equation for the second moment of the flux (i.e., the spatial correlation function/clusters) pops back in the mean field equation (for the flux).

It is also important to notice that the flux mean field equation has a different form than the cosine shape solution of the one-group criticality diffusion equation, explaining thus qualitatively the biases observed in Fig. 5. This can nicely be interpreted as follows: far from the boundaries, the soliton wave of our cluster averages so as to produce a flat density profile. Near the boundaries, the leakages are big and are therefore compensated by a very strong splitting of neutrons required to keep the overall mass constant. This produces a reflection of the whole wave on the boundary, explaining that the lower the number of neutrons, the flatter the distribution (even near the edges of our system). Ultimately, this pledges in favor of a bias on local tallies proportional to $1/N$ since the spatial correlation function has the same dependence on the overall number of particles.

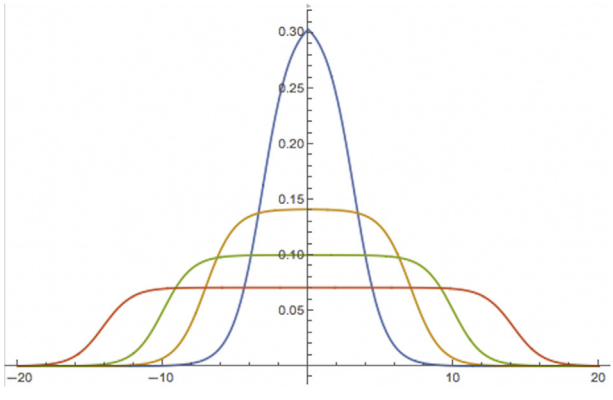

Fig. 7. Neutron density as a function of the position x as given by Eq. (21) with $\beta = 1$, up to different observation time (from the blue curve to the red curve as time goes by).

5. Conclusions

By resorting to a generalized Fisher-like equation with time-dependent coefficients that accounts for population control, we have successfully built a stochastic model able to reproduce undersampling biases observed in the Monte Carlo criticality simulation of loosely coupled systems and large reactor cores. An asymptotic analysis of this equation made it possible to study the dynamics of the neutron field emerging from clustered population of neutrons. We have shown that this field obeys a traveling wave equation, and we have postulated that clusters (described by the spatial correlation function) should have a soliton wave dynamic. We have also shown that the biases arising in Monte Carlo criticality simulation of decoupled systems can be understood as arising from spatial correlations and neutron clustering combined with leakage boundary conditions. Since the clustering amplitude has been shown to be bounded by $\frac{2}{3}\frac{\beta}{\gamma}\frac{\nu_2}{N}\frac{L^2}{D}$, we predict that the bias on the local tallies should also be proportional to L^2 and inversely proportional to N. This explains precisely the observations on the bias on local tallies (Fig. 3). In a future work we will confirm this prediction on the bias on local tallies and we will present a variance reduction scheme which allows us to deal with this clustering effect, in order to get rid of the undersampling bias.

Conflicts of interest

There is no conflict of interest.

Acknowledgments

The authors wish to acknowledge Andrea Zoia and Alain Mazzolo for fruitful discussions.

References

[1] I. Lux, L. Koblinger, Monte Carlo Particle Transport Methods: Neutron and Photon Calculations, CRC Press, Boca Raton, 1991.
[2] H. Rief, H. Kschwendt, Reactor analysis by Monte Carlo, Nuc. Sci. Eng. 30 (1967) 395–418.
[3] J.J. Duderstadt, L.J. Hamilton, Nuclear Reactor Analysis, Wiley, New York, 1976.
[4] F. Brown, LA-UR-05-4983, Los Alamos National Laboratory, 2005.
[5] F. Brown, Proceedings of M&C2009, Saratoga Springs, N, USA, 2009.
[6] E.M. Gelbard, R. Prael, Computation of standard deviations in eigenvalue calculations, Prog. Nucl. Energy 24 (1990) 237.
[7] O. Jacquet, R. Chajari, X. Bay, A. Nouri, L. Carraro, Eigenvalue uncertainty evaluation in MC calculations using time series methodologies, in: Proceedings of the International Conference on Radiation Shielding, Lisbon, 2000.
[8] E. Dumonteil, F. Malvagi, Automatic treatment of the variance estimation bias in TRIPOLI-4 criticality calculations, in: "Proceedings of ICAP2012," Chicago, 2012.
[9] T. Ueki, F. Brown, D.K. Parsons, D.E. Kornreich, Autocorrelation and dominance ratio in Monte Carlo criticality calculations, Nucl. Sci. Eng. 145 (2003) 279.
[10] T. Ueki, F. Brown, D.K. Parsons, J.S. Warsa, Time series analysis of Monte Carlo fission sources: dominance ration computation, Nucl. Sci. Eng. 148 (2004) 374.
[11] W.R. Young, A.J. Roberts, G. Stuhne, Reproductive pair correlations and the clustering of organisms, Nature 412 (2001) 328.
[12] B. Houchmandzadeh, Clustering of diffusing organisms, Phys. Rev. E 66 (2002) 052902.
[13] B. Houchmandzadeh, Neutral clustering in a simple experimental ecological community, Phys. Rev. Lett. 101 (2008) 078103.
[14] B. Houchmandzadeh, Theory of neutral clustering for growing populations, Phys. Rev. E 80 (2009) 051920.
[15] E. Dumonteil, T. Courau, Dominance ratio assessment and Monte Carlo criticality simulations: dealing with high dominance ratio systems, Nucl. Technology 172 (2010) 120.
[16] E. Dumonteil, F. Malvagi, A. Zoia, A. Mazzolo, D. Artusio, C. Dieudonné, C. de Mulatier, Particle clustering in Monte-Carlo criticality simulations, Ann. Nuc. Energy 63 (2014) 612–618.
[17] A. Zoia, E. Dumonteil, A. Mazzolo, C. De Mulatier, A. Rosso, Clustering of branching Brownian motions in confined geometries, Phys. Rev. E 90 (2014)

042118.
[18] C. De Mulatier, E. Dumonteil, A. Rosso, A. Zoia, The critical catastrophe revisited, J. Stat. Mech. 15 (2015) P08021.
[19] J.T. Cox, D. Griffeath, Ann. Probab. 13 (1985) 1108–1132.
[20] T. Sutton, Anomalous behavior of Monte Carlo uncertainties near reflecting boundaries, in: Proceedings of the SNA+MC2013 conference, Paris, France, 2014.
[21] T. Sutton, Application of a discretized phase space approach to the analysis of Monte Carlo uncertainties, Nuc. Sci. Eng. 185 (2017) 174–183.
[22] G. Radulescu, D. Mueller, J. Wagner, Sensitivity and uncertainty analysis of commercial reactor criticals for burnup credit, Nucl. Technology 167 (2) (2009) 268–287.
[23] B. Cochet, A. Jinaphanh, L. Heulers, O. Jacquet, Capabilities overview of the MORET 5 Monte Carlo code, Ann. Nucl. Energy 82 (2015) 74–84.
[24] K.B. Athreya, P.E. Ney, Branching Processes, Grundlehren Series, Springer-Verlag, New York, 1972.
[25] G.I. Bell, S. Glasstone, Nuclear Reactor Theory, Van Nostrand Reinhold Company, New York, 1970.
[26] T.M. Sutton, A. Mittal, Neutron clustering in Monte Carlo iterated-source calculations, in: Proceedings of the M&C 2017 Conference, Jeju, South Korea, 2017.
[27] Y.-C. Zhang, M. Serva, M. Polikarpov, Diffusion reproduction processes, J. Stat. Phys. 58 (1990) 849–861.
[28] M. Meyer, S. Havlin, A. Bunde, Clustering of independently diffusing individuals by birth and death processes, Phys. Rev. E 54 (1996) 5567.
[29] R. Fisher, The wave of advance of advantageous genes, Ann. Eugen. 7 (1937) 355–369.
[30] A. Kolmogorov, I. Petrovskii, N. Piskunov, Study of the diffusion equation with growth of the quantity of matter and its application to a biology problem, Moscow University Mathematics Bulletin 1 (1937) 1–25.
[31] D.A. Birch, W.R. Young, A master equation for a spatial population model with pair interactions, Theor. Popul. Biol. 70 (2006) 26–42.
[32] T.J. Newman, E.B. Kolomeisky, J. Antonovics, Population dynamics with global regulation: the conserved Fisher equation, Phys. Rev. Lett. 92 (2004) 228103.